

---

## Sensor network and inertial positioning hybridisation for indoor location and tracking applications

---

Yuri Álvarez López\*, Guillermo Álvarez Narciandi and Fernando Las-Heras Andrés

Area of Signal Theory and Communications (TSC-UNIOVI),  
Department of Electrical Engineering,  
University of Oviedo,  
Edificio Polivalente, Módulo 8,  
Campus Universitario de Gijón,  
33203 Gijón (Asturias), Spain  
Email: yalopez@tsc.uniovi.es  
Email: ganarciandi@tsc.uniovi.es  
Email: flasheras@uniovi.es  
\*Corresponding author

**Abstract:** An indoor location system (ILS) for practical asset and people tracking in indoor scenarios using received signal strength (RSS) ZigBee-based sensor network and inertial sensors is presented. A novel algorithm that uses differential signal levels gathered from a set of transmitter nodes is developed for processing RSS data. These levels are introduced into a cost function whose minimum gives the asset location estimation. The use of differential field levels-based algorithm avoids the need of system calibration due to signal strength fluctuation. Moreover, position accuracy is improved by adding inertial sensor information. The method is tested in a real scenario, demonstrating practical indoor positioning when combining ZigBee-based sensor network and inertial sensors information. The influence of the number of ZigBee nodes on the position estimation accuracy has been analysed.

**Keywords:** WSN; wireless sensor networks; ILS; indoor location systems; RSS; received signal strength; zigBee; inertial sensors; radio determination.

**Reference** to this paper should be made as follows: López, Y.Á., Narciandi, G.Á. and Andrés, F.L-H. (xxxx) 'Sensor network and inertial positioning hybridisation for indoor location and tracking applications', *Int. J. Sensor Networks*, Vol. x, No. x, pp.xxx-xxx.

**Biographical notes:** Yuri Álvarez López received his MS and PhD in Telecommunication Engineering from the University of Oviedo, Gijón, Spain, in 2006 and 2009, respectively. He is currently an Associate Professor at the Signal Theory and Communications TSC-UNIOVI research group of the University of Oviedo, Spain. He received the 2011 Regional and National Awards to the Best PhD Thesis on Telecommunication Engineering (Category: Security And Defence).

Guillermo Álvarez Narciandi received his BS in Telecommunication Technologies and Services Engineering from the University of Oviedo, Gijón, Spain, in 2014. He is currently a student of the MS in Telecommunication Engineering of the University of Oviedo, Spain. He received his 2015 EPIGIJON Industrial Partners Society Award to the Best Applied Project for the development and testing of a hybrid RSS-inertial Indoor Positioning System.

Fernando Las-Heras Andrés received his MS in 1987 and the PhD in 1990, both in Telecommunication Engineering, from the Technical University of Madrid. Currently he is a Full Professor and the Principal Investigator of the Signal Theory and Communications TSC-UNIOVI Research Group of the University of Oviedo, Spain. From 2005 to 2015 he held the Telefónica Chair ICTs and Smart Cities at the University of Oviedo.

---

### 1 Introduction

In the last few years, the need for new wireless methods for people and asset tracking has made indoor location systems

(ILS) to become a major research topic (Farid et al., 2013). This interest comes after the popularisation of global positioning system (GPS), which provides accurate outdoor

location. However, GPS is not operative inside buildings and industrial warehouses as there is no line-of-sight between the antenna and satellites.

In Farid et al. (2013), ILS is defined as any system that provides a precise position inside a closed structure, as for example, industrial warehouses, public buildings (hospitals, schools, airports), flats and condominiums, etc. A number of ILSs have been proposed in the literature, based on infrared signals, ultrasound, inertial sensors and radiofrequency mainly, as summarised in Table 3 of Farid et al. (2013) and Table 1 of Shirehjini et al. (2012), with location accuracy ranging from 0.5 m to 5 m for the compared methods. The latter are, in general, range-based distance measurements systems, which can be classified in two main groups: time-of-flight (ToF) and received signal strength (RSS). On the one hand, ToF (Macii et al., 2013) is based on the signal propagation time between a transmitter (Tx) and a receiver (Rx) node. On the other hand, RSS techniques (e.g., Álvarez et al., 2011; Bandara et al., 2004; Chen et al., 2015; Gomes and Sarmiento, 2009; Huang et al., 2015; Ismail et al., 2008; Macii et al., 2013), use the measured signal strength information converting it into distance.

Radiofrequency-based ILS network infrastructure mainly consists of a set of anchor or static nodes, deployed in the scenario under test, and mobile nodes tagged to the assets to be tracked. One (either the static or the mobile) has to be configured as transmitter, and the other as receiver.

ILS deployment for a particular scenario is affected by the following criteria:

- 1 size of the scenario where the ILS is deployed
- 2 positions where static nodes can be placed
- 3 required location accuracy
- 4 the environment where the ILS is deployed (office building, industrial warehouse, shop store)
- 5 number of assets to be tracked
- 6 the response/refreshing time of the ILS.

With respect to the two latter criteria, ILSs can track several assets or people at the same time. However, when working with more than one mobile node, the RSS data acquisition time must be split according to the total number of tracked mobile nodes in order to be able to get the information of each node (identifier, ToF or RSS value), then setting a trade-off between the response of the ILS and the number of assets to be monitored.

Accuracy will depend mainly on the static nodes density. Thus, for a given accuracy, one can calculate the minimum number of static nodes. In practical applications, the number of static nodes will be oversized to guarantee the requested accuracy with the highest probability.

RSS-based ILS processing algorithms can be classified in three main groups:

- 1 fingerprinting (Chen et al., 2013; Hossain et al., 2007; Ismail et al., 2008)

- 2 empirical models (Bandara et al., 2004; Gomes and Sarmiento, 2009; Jiménez-Ruiz et al., 2012; Pivato et al., 2011)
- 3 theoretical free-space path loss (also known as free space propagation) (Álvarez et al., 2011; Huang et al., 2015; Ismail et al., 2008; Macii et al., 2013).

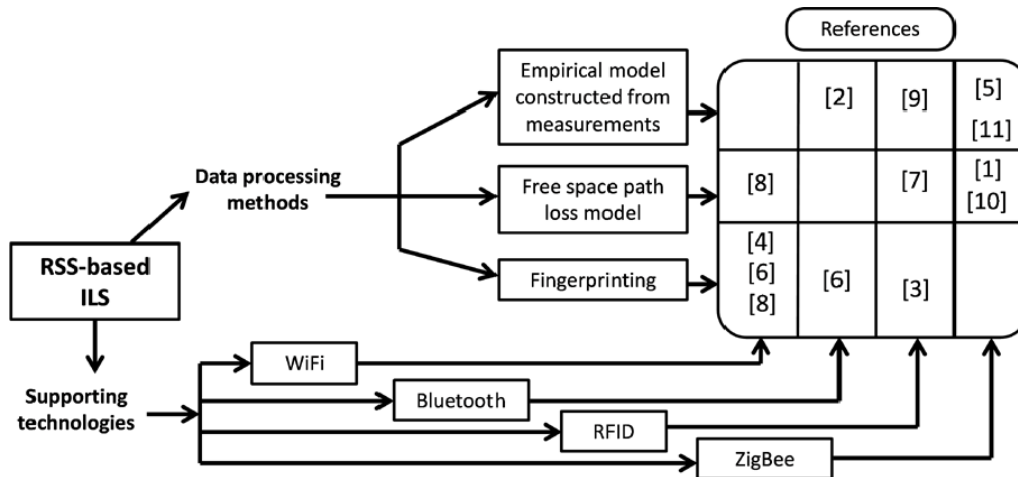
In the case of fingerprinting and empirical models, a previous characterisation of the ILS deployment scenario is required. This characterisation consists of RSS measurements in a set of points in such scenario, aiming to create a RSS database (fingerprinting) or to use them as inputs for a regression model (empirical model). Free-space path loss model does not require such previous time-consuming measurement stage, although depending on the ILS algorithm implementation, ILS calibration can be done to get rid of systematic errors (e.g., different sensitivity of each static node).

Fingerprinting has been proved to be more accurate than free-space path loss model (Table 3 of Farid et al., 2013; Table 1 of Shirehjini et al., 2012). However, it is quite sensitive to variations in the scenario under test. For example, if furniture were moved within the scenario, fingerprinting database would have to be generated again to keep the accuracy. To sum up, RSS-based ILS classification according to supporting technologies and data processing methods is depicted in Figure 1.

In spite of the different nature of the aforementioned RSS data processing techniques, the achieved RSS-based ILS position estimation accuracy is, in general, in the same order of magnitude for a given scenario and ILS parameters (mainly the static nodes density, i.e., number of static nodes per surface unit). In all the cases, multi-path propagation is the main source of error causing measured RSS values to fluctuate: the signal is reflected in obstacles, then creating multiple propagation paths that may cause interference.

Nowadays, the most common technologies for the deployment of RSS-based ILS are ZigBee (Álvarez et al., 2011; Gomes and Sarmiento, 2009; Macii et al., 2013; Pivato et al., 2011; Tennina et al., 2009), WiFi (Gallagher et al., 2012; Hossain et al., 2007; Ismail et al., 2008), Bluetooth (Bandara et al., 2004; Hossain et al., 2007), and RFID (Huang et al., 2015; Jiménez-Ruiz et al., 2012), with the latter growing rapidly due to the low price of RFID tags. ZigBee is more suitable than RFID or WiFi for the deployment of a sensor network thanks to features such as low power consumption of ZigBee nodes, and ease of connection with sensing devices (gas, temperature, humidity) and actuators.

ZigBee nodes (both static and mobile) have the same hardware features: operating mode can be set by software. RFID networks consist of readers (static) and tags (mobile), the former being quite more expensive than the latter. Thus, depending on the final application (kind of scenario, number of assets to be tracked), either ZigBee or RFID could be the most advantageous even in terms of cost.

**Figure 1** Classification of RSS-based ILS according to data processing methods and supporting technologies

Source: [1] Álvarez et al. (2011), [2] Bandara et al. (2004), [3] Chen et al. (2015), [4] Gallagher et al. (2012), [5] Gomes and Sarmento (2009), [6] Hossain et al. (2007), [7] Huang et al. (2015), [8] Ismail et al. (2008), [9] Jiménez-Ruiz et al. (2012), [10] Macii et al. (2013) and [11] Pivato et al. (2011)

The rapid popularisation of portable devices such as PDA, tablets, laptops, which include connectivity via Bluetooth and/or WiFi protocols, have attracted interest for ILS developers, based on the fact that the hardware infrastructure is already deployed (Ismail et al., 2008). In the case of WiFi, static nodes are the access points (AP), and portable devices act as mobile nodes. Bluetooth-based ILS infrastructure mainly consists of Bluetooth beacons usually acting as static nodes, and portable devices equipped with Bluetooth connection for mobile nodes.

Another different approach for ILS is based on inertial sensors systems (Gallagher et al., 2012; Jiménez-Ruiz et al., 2012). They are also referred as dead reckoning systems, that is, self-contained methods which do not rely on any external infrastructure. The inertial sensors, accelerometers and gyroscopes which measure, respectively, linear acceleration and angular rotation, form the inertial measurement unit (IMU). From a given initial position and using the information of those signals, it is possible to update the position of the object (Jiménez-Ruiz et al., 2012). Hence, inertial systems are not affected by the inherent issues of signal propagation of other location systems (multipath mainly). Besides, position and orientation calculation do not need external references, thus avoiding the need for a network of static nodes deployment. The main drawback of this type of navigation is the error drift: estimated position error grows each time the position is updated and thus, accurate sensors are needed. This drawback can be also overcome by combining inertial sensors with another ILS capable to provide a reference position, as proposed in Jiménez-Ruiz et al. (2012), by combining the information given by the IMU with an RFID-based ILS.

The development of microelectromechanical systems (MEMS) technology has made inertial sensors smaller and cheaper. Their accuracy, which used to be very low with

this technology, has been enhanced enabling the use of low cost IMUs.

This work follows the idea of Jiménez-Ruiz et al. (2012), where inertial sensor information is combined with RSS data to correct the main sources of error of each one: drift in inertial sensor, and multipath in RSS. Instead of using RFID as in Jiménez-Ruiz et al. (2012), the idea is to extent RSS-based ILS, conceived for assets location and tracking, using ZigBee such as Álvarez et al. (2011) and Gomes and Sarmento (2009). The novelties of the current contribution with respect to Álvarez et al. (2011) and Gomes and Sarmento (2009) are:

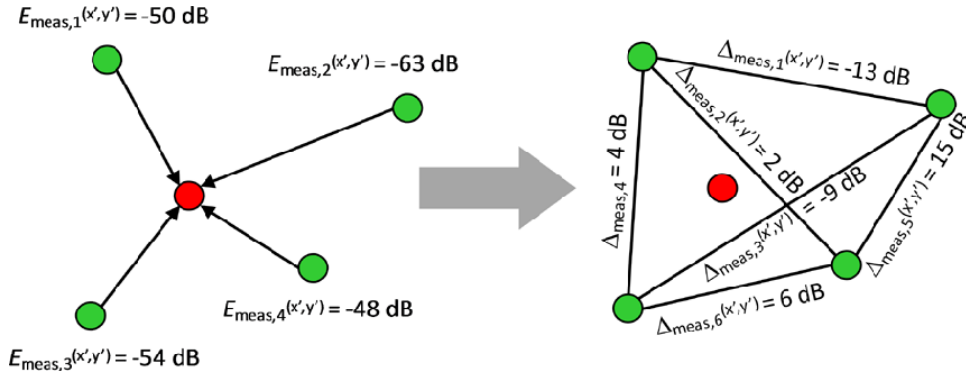
- A novel RSS algorithm that uses differential field levels of the radiolinks between each transmitting node and receiving node, thus avoiding an initial calibration stage of the system as well as periodic recalibration due to signal strength fluctuations or modification of the scenario where the ILS is deployed.
- Development of a hybrid ZigBee–inertial sensor-based system for asset location and tracking, tested in a real indoor scenario.

## 2 Indoor location system description

### 2.1 Received signal strength-based location algorithm

From a practical point of view, the role of transmitter and receiver nodes can be either assigned to the static or mobile nodes, thanks to the wireless channel propagation reciprocity between transmitter and receiver. In the application example presented in this work, the mobile node will be configured as receiver and the static nodes as transmitters (as depicted in Figure 2). Thus, for the sake of simplicity, the formulation presented in this section will follow this convention.

**Figure 2** Idea of RSS-based ILS using absolute (left) and differential (right) field levels. Green dots: static nodes. Red dot: mobile node (see online version for colours)



In general, RSS-based ILS techniques (Sklar, 2001) make use of the free space propagation exponential<sup>1</sup> decay law (1) for the radiolinks between static and mobile devices or nodes:

$$E_{Rx} = E_{ref} (\lambda / 4pR), \quad (1)$$

where  $E_{Rx}$  is the field at the receiver (mobile node).  $E_{ref}$  is a reference field level, usually evaluated at the static nodes (transmitter nodes) during a calibration stage and  $\lambda$  is the signal wavelength. It is assumed that mobile and static nodes are placed at the positions  $(x', y')$  and  $(x, y)$ , respectively, considering that  $z \approx z'$ . Thus, the distance between a mobile node and a static node is (2):

$$R = ((x - x')^2 + (y - y')^2)^{1/2}. \quad (2)$$

To improve the propagation model, equation (3) of Álvarez et al. (2011) includes quadratic and cubic field decay terms in the propagation model. From its representation shown in Figure 1 of Álvarez et al. (2011), a sharp variation around the distance from which the term  $1/R$  is dominant is observed. However, typical measured signal strength decay does not exhibit a variation as sharp as predicted by equation (3) of Álvarez et al. (2011). A better propagation model, exhibiting smoother transition, is achieved by means of:

$$E_{Rx} = E_{ref} ((\lambda / 4pR) + (\lambda^2 / 8p^2R^2) + (\lambda^3 / 16p^3R^3)). \quad (3)$$

Depending on the selected working frequency, quadratic and cubic field decay terms may be negligible at a distance of few centimetres far from the transmitter (Álvarez et al., 2011).

The location problem aims to determine the mobile position coordinates  $(x', y')$  from the RSS values corresponding to the set of  $N$ -static nodes whose positions  $(x_n, y_n)$  are known. For this goal, the following cost function is established (Álvarez et al., 2011):

$$f_{\text{cost\_ant}}^{(x',y')} = \sum_{n=1:N} |E_{\text{teor},n}^{(x',y')} - E_{\text{meas},n}^{(x',y')}|^2. \quad (4)$$

$E_{\text{teor},n}^{(x',y')}$  is the theoretical field level at the position  $(x', y')$  radiated by the  $n$ th static node, which is calculated using equation (3) ( $E_{\text{teor},n}^{(x',y')}$  is  $E_{Rx,n}$  in equation (3)).  $E_{\text{meas},n}^{(x',y')}$  is the

measured field level at the position  $(x', y')$  emitted by the  $n$ th static node.

The mobile node position  $(x', y')$  is the unknown. Thus, the cost function (4) has to be evaluated in a set of points  $(x', y')$  that belong to the scenario under test, for example, the points of a regular grid in which the scenario under test is discretised. The mobile node position estimation is associated to the  $(x', y')$  point that corresponds to the minimum cost function value.

One major problem of the cost function (4) is that absolute field values,  $E_{ref}$ , are involved, thus requiring calibration of the ILS when deployed in a new scenario. Furthermore, transmitted field levels may vary with environmental conditions, so periodic calibration may be required to ensure proper ILS system operation.

To avoid the need of calibration (i.e. the determination of the value of  $E_{ref}$ ), this contribution proposes a new cost function that makes use of differential field levels. The concept is depicted in Figure 2: first, the field level difference between a pair of static nodes is calculated, for both theoretical ( $\Delta_{\text{teor}}$ ) and measured ( $\Delta_{\text{meas}}$ ) values (5):

$$\begin{aligned} \Delta_{\text{teor},m}^{(x',y')} &= |E_{\text{teor},p}^{(x',y')} - E_{\text{teor},q}^{(x',y')}|, \\ \Delta_{\text{meas},m}^{(x',y')} &= |E_{\text{meas},p}^{(x',y')} - E_{\text{meas},q}^{(x',y')}|, \end{aligned} \quad (5)$$

$$p = [1, 2, \dots, N-1]; \text{ for every } p: q = [p+1, \dots, N],$$

$$m = [1, 2, \dots, M], \text{ with } M = N(N-1)/2.$$

Then, a new cost function relating the theoretical ( $\Delta_{\text{teor}}$ ) and measured ( $\Delta_{\text{meas}}$ ) field level differences is established:

$$f_{\text{cost}}^{(x',y')} = \sum_{m=1:M} |\Delta_{\text{teor},m}^{(x',y')} - \Delta_{\text{meas},m}^{(x',y')}|^2 \quad M = N(N-1)/2. \quad (6)$$

As for equation (4), this cost function  $f_{\text{cost}}^{(x',y')}$  is evaluated in a set of points  $(x', y')$  belonging to the scenario under test. Hence, the mobile node position estimation is associated to the  $(x', y')$  point that yields the minimum cost function value.

The main advantage of the proposed cost function (6) is that differential field levels are used (i.e., the knowledge of  $E_{ref}$  is not required), so the position estimation will not be

affected by signal strength drift, provided the  $N$  static nodes have the same power emission drift. The drawback of this method is that the amount of data,  $M$ , is proportional to the square of the number of static nodes  $N$ .

The scenario under test can be discretised in a regular grid of  $(x', y')$  positions, where the separation between adjacent  $(x', y')$  points can be set according to the required ILS accuracy. For a two-dimensional scenario, evaluating cost function (4) or (6) at several thousands of  $(x', y')$  positions can be done in few milliseconds with a conventional laptop, so the ILS response time will eventually depend on the RSS acquisition rate (mainly limited by the supporting hardware). As mentioned in Section 1, tracking more than one mobile asset will increase that response time.

### 2.2 ZigBee network implementation

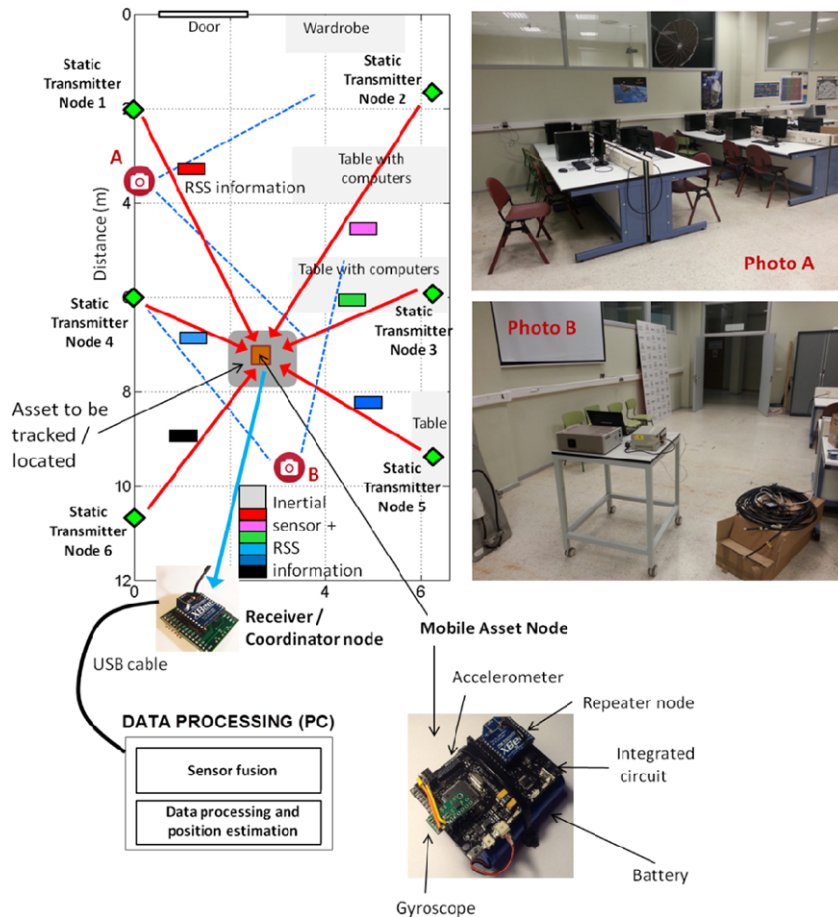
Among the different possibilities for hardware implementation of the ILS, ZigBee nodes operating at 2.45 GHz were selected due to their reasonable cost, widespread utilisation and multiple configuration options; and above all, ZigBee has been conceived as a low power requirement wireless sensor network, suitable for the proposed ILS application (Álvarez et al., 2011; Gomes and Sarmiento, 2009; Macii et al., 2013; Pivato et al., 2011). Besides, ZigBee routing capabilities are suitable to

forward RSS information to the device that runs the location algorithm, without requiring additional network infrastructure, unlike RFID, where the readers have to be connected using another network technology. In addition to this, the coverage of the ZigBee network could be extended beyond the coverage area of each individual static node (that ranges from 10 m to 20 m in indoor scenarios) by means of the inclusion of repeater nodes.

Three ZigBee node types, all based on the same IEEE 802.15.4 PHY link, are used in the network, as shown in Figure 3: first,  $N$  static or transmitting nodes are placed at known locations  $(x_n, y_n)$ . Second, the node attached to the mobile asset senses the RSS level received from the  $n$ th static node, gathers these RSS values, and forward them to the receiver/coordinator node. Last, the receiver node acts as interface between the ZigBee network and the computer. Commercial ZigBee modules operating at 2.4 GHz with 250 Kbps data rate including RSS indicator functionality have been used for the setup and measurements (XBee® ZigBee RF Modules, 2015).

The setup proposed for the ZigBee-based ILS system presented in this work collects RSS information every 500 ms, with a duty cycle of 2%, that is, nodes will be in sleep mode for 490 ms, and active during 10 ms. This 2% duty cycle is chosen as a trade-off between refreshing time (concerning tracking capabilities) and battery savings.

**Figure 3** ILS implementation using ZigBee network and inertial sensors in a real environment. Pictures of the  $12 \times 6$  m classroom room selected for testing the system. Camera icons mark the places where pictures were taken (see online version for colours)



### 2.3 Inertial system description

An accelerometer attached to an object measures, in each of its axis, the sum of the acceleration due to the object movement,  $a_t$ , and that of gravity,  $g$ . Hence, to compute the displacement of the object it is required to isolate the former acceleration from the undesired gravity components. For this purpose, it is necessary to rotate from the moving frame, defined by the accelerometer and the object or asset to be tracked, to an inertial frame in which the gravity is subtracted. This can be performed, using equation (7), multiplying the accelerometer measurements,  $a_m$ , by a rotation matrix which describes the Euler rotations,  $R_I^B$ , defined as the transpose of the matrix in equation (67) of Diebel (2006).

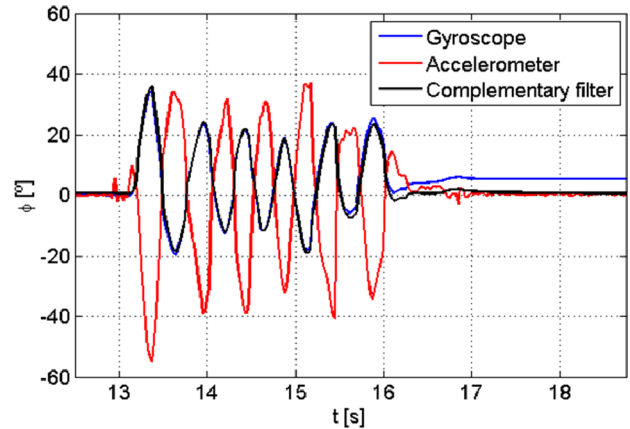
$$a_I = R_I^B a_m + (0 \ 0 \ g)^T \quad (7)$$

Therefore, as initial step, the orientation of the asset to be tracked must be computed. By fusing the data from the inertial sensors, a good estimate of the asset heading can be obtained. Hence, it is possible to compute the moving frame acceleration and integrate it twice to estimate the asset displacement from a reference point. The tested inertial system uses low-cost MEMS sensors: a tri-axial accelerometer LIS331DLH (Accelerometer LIS331DLH, 2015) and a tri-axial gyroscope L3GD20H (Gyroscope L3GD20H, 2015) whose measurements were combined with a complementary filter. The complementary filter coefficients are obtained by means of a frequency domain analysis. Thus, the gyroscope, whose measurements are integrated, follows high frequency variations while the accelerometer holds long-term tendency. To illustrate this, the computed pitch of the asset to be tracked during approximately 6 s is depicted in Figure 4. In this period of time, the asset is rotated several times to test the accelerometer output. The pitch of the asset computed with only the accelerometer data (red line) differs from the true pitch value when the asset is rotated. The blue line represents the pitch calculated with the gyroscope data, which is a reliable estimation of the true pitch value on the short term. However, as this value is obtained integrating gyroscope signals, it drifts with time. Finally, the pitch computed using the complementary filter (black line) provides accurate estimations of the true pitch angle value when the asset is rotated while it removes the drift. Several laboratory tests showed that the true pitch value could be considered equal to the pitch computed with the complementary filter.

Finally, once the orientation is computed, the Euler rotations are performed and the gravity is subtracted. The resulting data correspond to the moving frame acceleration, which is integrated twice in order to obtain the displacement between two consecutive samples. Figure 5 represents a simplified scheme of IMU data processing.

Both the accelerometer and the gyroscope are low-cost sensors with low power consumption. In addition, the complementary filter is very simple from a computationally point of view. This is critical for the autonomy of the repeater node attached to the asset to be tracked.

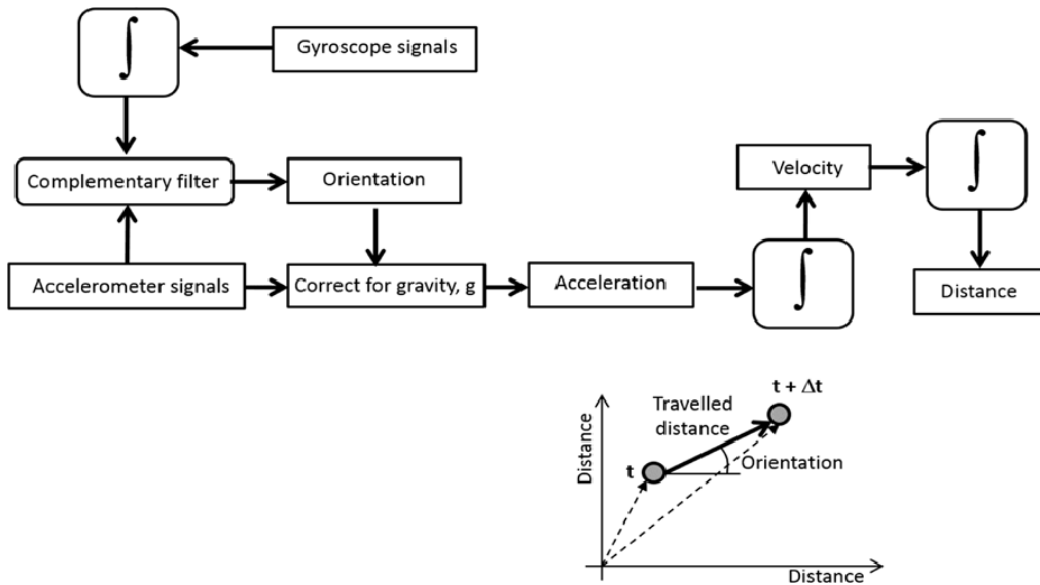
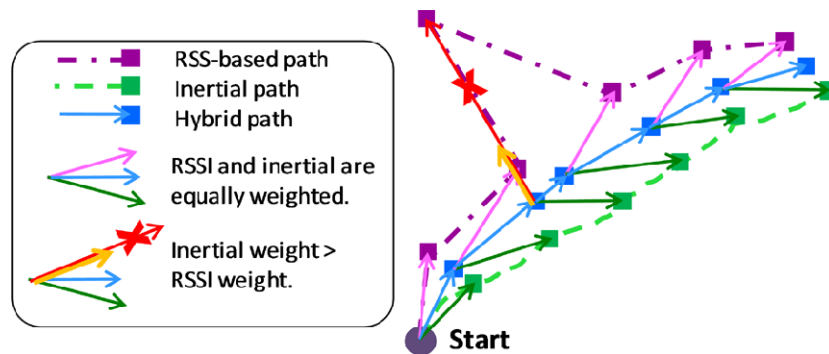
**Figure 4** Estimated pitch angle using accelerometer data (red line), gyroscope data (blue line) and combining both with a complementary filter (black line) (see online version for colours)



### 2.4 Inertial and RSS-based systems combination

As pointed out in Section 1, one of the goals of this research is to improve the RSS-based ILS location performance with inertial sensors information.

While the RSS-based system takes samples every 500 ms, inertial sensors update information every 25 ms. In the case of the RSS-based system, the choice of the sampling rate was made considering a trade-off between the power consumption of the nodes and the tracking capabilities of the system. Since a buffer of 10 samples is considered in order to smooth the trajectory mitigating multipath effects, it is necessary to take new samples fast enough not to filter out the trajectory of the asset to be tracked. In the case of the inertial system, a higher sampling rate is required in order not to lose information of the movement of the object and thus achieve a good performance. This data can be processed and stored in an integrated circuit attached to the asset to be tracked in order to send it in ZigBee frames with the RSS data to the receiver node. Thus, the asset position is reestimated each time the inertial sensors are sampled. When the RSS-based system collects a new set of samples (i.e., every 500 ms), the information of both systems is combined. Linear regression is used to fit the inertial samples taken between two RSS data acquisitions, filtering noise and vibration. Next, displacement vectors are constructed from two consecutive inertial and RSS datasets, as shown in Figure 6: green arrows represent inertial displacement and the pink arrows represent RSS displacement.

**Figure 5** Inertial system signals processing for orientation and distance calculation**Figure 6** Example of inertial sensor and RSS data fusion. Schematic representation of information weighting. Squares indicate points where data is combined and position is calculated (see online version for colours)

Even though a moving average buffer is applied to RSS values, they can still exhibit abnormal signal variation, reflected in RSS-based position estimation. These significant path fluctuations can be easily detected if compared with previous RSS and inertial displacement vectors variation. If the current displacement is not larger than twice the previous displacement values, RSS and inertial vectors are equally weighted. Otherwise, RSS displacement vector weight is inversely proportional to RSS distance variation excess, as depicted in Figure 6 (red and yellow arrows).

### 3 Validation

This section is devoted to experimentally evaluate the performance of the proposed ILS in a real scenario. The ILS design criteria are:

- 1 size of the scenario where the ILS is deployed: a  $12 \times 6 \text{ m}^2$  classroom
- 2 positions where static nodes can be placed: walls of the classroom (shown in Figure 3)

- 3 required location accuracy: this criterion is the one to be analysed, so it cannot be defined a priori
- 4 environment where the ILS is deployed: a classroom with furniture (tables, wardrobes, chairs, computers)
- 5 number of assets to be tracked: one
- 6 response/refreshing time of the ILS: 500 ms (ZigBee nodes sampling rate).

The choice of this scenario size ( $12 \times 6 \text{ m}$ ) is motivated by the fact that it is similar to others used for ILS testing, some of them listed in Table 1, making easier the comparison of the evaluated ILS's.

To cope with RSS fluctuations inherent to indoor measurements due to multipath and time-varying scenario, a solution based on a moving average is considered. RSS values are stored in a 10-samples size 'first in–first out' (FIFO) buffer. The averaged RSS values are used to estimate the position of the asset. Taking into account that RSS samples are taken every 500 ms, a 10-samples size buffer introduces a 5 s delay (sufficient for the majority of slow-motion asset tracking applications) while keeping reasonable accuracy as it will be shown next.

**Table 1** RSS-based ILS comparison sorted by maximum relative error (% of the scenario size)

<i>Method</i>	<i>Scenario size (m)</i>	<i>No. static nodes, N</i>	<i>Absolute error</i>	<i>Relative error (%)</i>
Hybrid inertial and RFID system (Jiménez-Ruiz et al., 2012)	60 × 40 1000 m path	71	11.5 m (in a 1000 m path)	1.1% (in a 1000 m path)
This work (RSS + inertial)	12 × 6	6	Up to 0.7 m	Up to 5.2%
RSS-based RFID (Huang et al., 2015)	10 × 5	6	0.83 m	7.4%
Data fusion (RSSI and ToF), ZigBee (Macii et al., 2013). Range estimation only	5 × 5 m	1	Around 50–60 cm. Up to 1 m	Around 50–60 cm. Up to 14% m
RSS-based ZigBee (Álvarez et al., 2011)	12 × 6	6	0.5 m avg. Up to 2 m	3.7% avg. Up to 15%
This work (RSS-only)	12 × 6	6	Up to 2.1 m	Up to 16%
RSS-based WiFi, fingerprinting (radiomap) (Ismail et al., 2008)	7.4 × 14 m	3	Up to 2.5 m	16% (80% certainty)
Fingerprinting, RSS-based WiFi and Bluetooth (Hossain et al., 2007)	540 m <sup>2</sup> 23 × 23 m approx.	4 (62 train. pts)	5 m (90% certainty)	21% (90% certainty)
RSS-based ZigBee, centroid concept-based algorithms (Pivato et al., 2011)	5.8 × 4 m	12	Around 2 m (90% certainty)	Around 28% (90% certainty)
RSS-based Bluetooth (Bandara et al., 2004)	4.5 × 5.5 m	4	2 m (92% certainty)	28% (92% certainty)
This work (RSS-only)	12 × 6	4	Up to 3.8 m	Up to 28%
RSS-based ZigBee, WAF model (Gomes and Sarmiento, 2009)	3.5 × 6.1 m	4	Up to 2.5 m	35%

### 3.1 Comparison of absolute and differential field levels

First, a comparison between ILS accuracy using absolute RSS (equation (4)) plus a previous calibration stage, and differential RSS (equation (6)) (without calibration stage) is presented. For this comparison, 20 static positions within the classroom have been randomly selected. For each position, 100 RSS acquisitions were conducted, one every

500 ms (so the overall acquisition time for each position is 50 s). During the acquisition time, two people were walking inside the classroom aiming to create a time-varying environment. The number of active static nodes has also been evaluated for each of the two compared cost functions. ILS accuracy is assessed by means of the following indicators: mean error, maximum error, standard deviation and the radius of the dispersion circle (DC). The latter is defined as the radius of the maximum circle that contains all the estimated target locations for a fixed position.

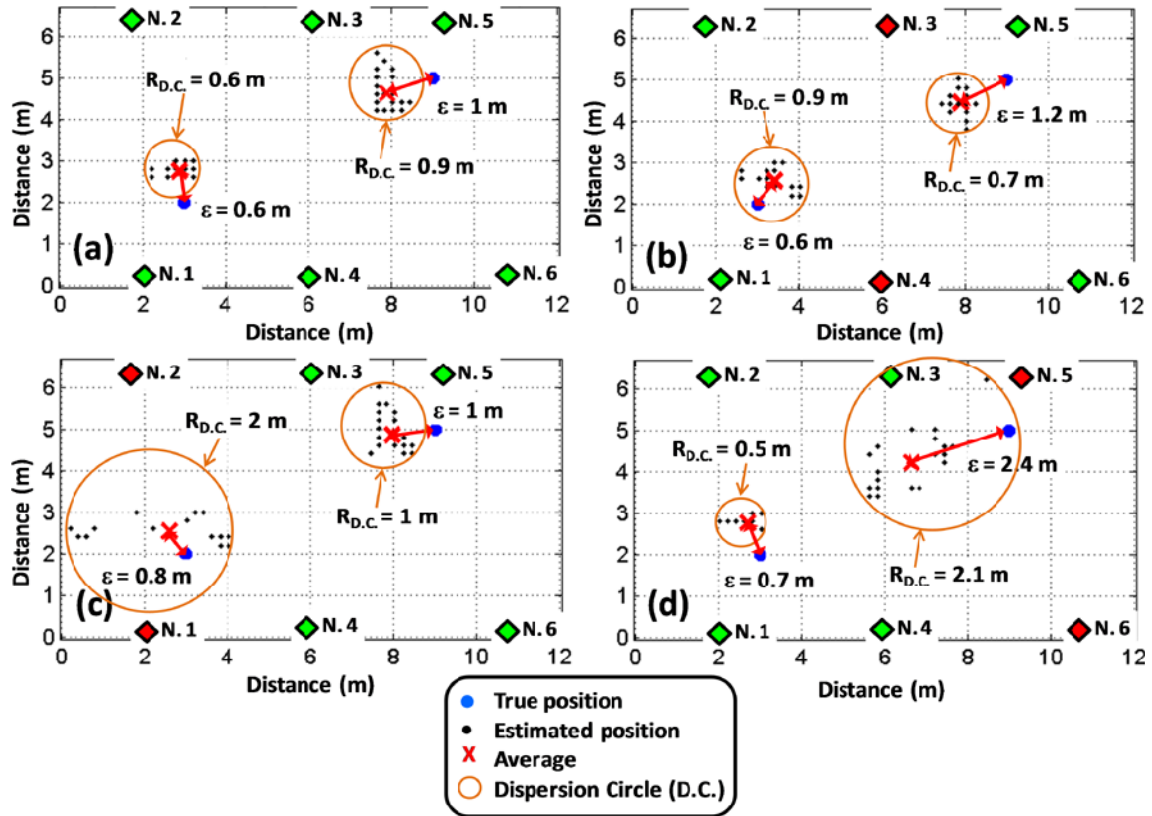
Results for different sets of active nodes as well as the processing technique (absolute RSS + calibration, equation (4); and differential RSS, equation (6)) are summarised in Table 2. Besides, location estimation using equation (6) (differential RSS) for several sets of nodes and static positions are depicted in Figure 7, illustrating the concept of DC.

From Table 2, it can be noticed that there is not significant improvement when using the differential RSS method with respect to the technique based on absolute RSS values plus calibration stage. Concerning the number of nodes, the accuracy of the RSS-based system is around 1 m with dispersion smaller than 0.7 m using six nodes. If only four nodes were considered, accuracy is worsened up to 1.6 m, as well as the dispersion (around 1.2 m). The influence of the nearest static nodes to the true position of the mobile node (blue dot) can be also observed in Figure 7: when the nearest nodes are deactivated, the dispersion is significantly worsened in this real-time varying scenario.

**Table 2** Analysis of the RSS-based ILS uncertainty for different number of nodes and location technique

<i>No. of nodes, N (list of active nodes)</i>	<i>Method</i>	<i>Mean error</i>	<i>Maximum error</i>	<i>Standard deviation</i>	<i>Radius dispersion circle (R<sub>D.C.</sub>) (m)</i>
		<i>(m)</i>	<i>(m)</i>	<i>(m)</i>	
N = 6 [1,2,3,4,5,6]	Differential RSS	1.1	2.1	0.6	0.7
	Absolute RSS + calibration	1.2	2.1	0.8	0.6
N = 4 [1,2,5,6]	Differential RSS	1.5	3.4	1.5	1.0
	Absolute RSS + calibration	1.5	3.3	1.7	1.2
N = 4 [3,4,5,6]	Differential RSS	1.7	3.6	1.5	1.4
	Absolute RSS + calibration	1.6	3.2	1.6	1.3
N = 4 [1,2,5,6]	Differential RSS	1.6	3.5	1.3	1.2
	Absolute RSS + calibration	1.8	3.8	1.4	1.3

**Figure 7** Analysis of positioning uncertainty with RSS information for selected static positions (blue dots). Different set of static nodes are activated (green diamonds): (a) all static nodes activated; (b) nodes 3 and 4 deactivated; (c) nodes 1 and 2 deactivated and (d) nodes 5 and 6 deactivated (see online version for colours)



### 3.2 RSS-based ILS combined with inertial systems

Once the RSS-based ILS performance has been evaluated, next step is devoted to test the position accuracy improvement achieved when combining RSS and inertial sensor information. Inertial sensors require the asset to be in motion, so a path has been created in the scenario under test, shown in Figures 8 and 9 (thick orange line).

Path estimation for 4 and 6 static nodes are depicted in Figures 8 and 9, respectively. The path computed by the RSS-based method (dash-dotted purple line) has the lowest accuracy among the three systems under study with a maximum error of 2.1 m in the case of four nodes (Figure 8) and 1.7 m, when considering six static nodes (Figure 9). This maximum position estimation error, which does not occur at the intermediate testing positions marked (with geometric shapes) in Figures 8 and 9, is in agreement with Table 2 results.

As mentioned in Jiménez-Ruiz et al. (2012), inertial-based tracking systems suffer from error drift, meaning that the positioning error steadily increases as the asset to be tracked moves along the path. In this example, if the initial position is assumed to be known, the

inertial system positioning error at the end of the path is 0.6 m.

In practice, inertial-based systems require the initial position of the asset to be given. For example, in this work the initial position is estimated by the RSS-based ILS, as depicted in Figures 8 and 9 (dashed green line). Note that this RSS-based initial position estimation is different for Figures 8 and 9, and so the inertial system positioning error with respect to the true path.

Next, RSS and inertial sensor information are combined. The estimated path (solid blue line) follows closely the true path of the mobile node, reducing RSS-based uncertainty as well as the inertial system drift. Path error is up to 1.2 m when four static nodes are considered (Figure 8), and up to 0.5 m with six static nodes.

Additional paths have been created and evaluated in the scenario, achieving the following metrics ( $N = 6$  static nodes deployed): for the inertial system, the error drift at the end of the path is within the range [0.5–0.8] m (initial position is assumed to be known for this analysis); RSS-based technique provides a maximum positioning error of [1.5–2.1] m; and combined RSS and inertial sensor information yields a maximum positioning error of [0.4–0.7] m.

**Figure 8** Tracking results for the RSS-based system, inertial system, and the hybrid system, when four nodes are active. The true path is highlighted in light orange. Initial position is denoted with (●), final position is denoted with (+), and intermediate positions are denoted with (■) and (★). Positioning errors for every tested location system are depicted (see online version for colours)

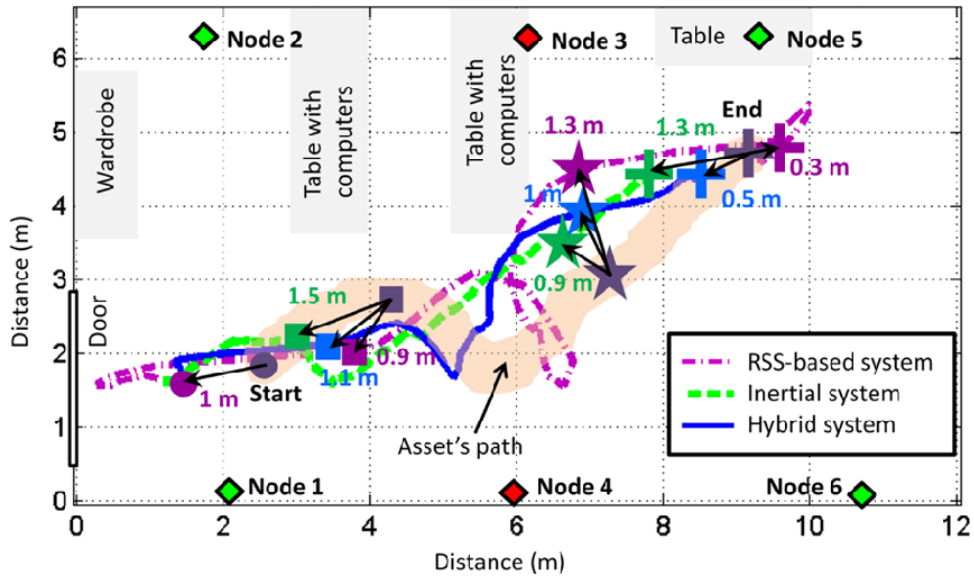
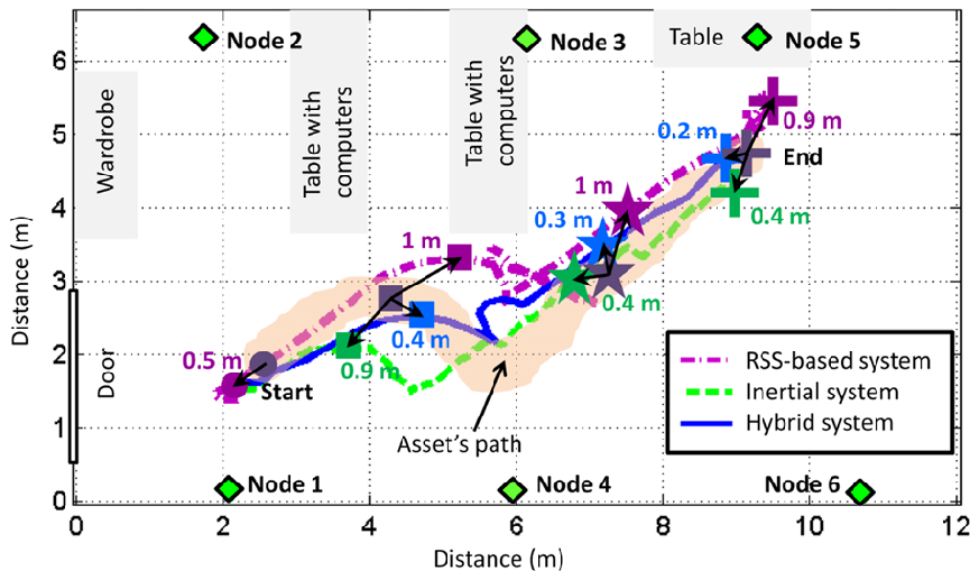


**Figure 9** Tracking results for the RSS-based system (dash-dotted purple line), inertial system (dashed green line), and the hybrid system (solid blue line), when the six nodes are active (see online version for colours)



#### 4 Conclusions

It can be concluded that, from the results considering just the RSS information, there is not significant improvement when using the differential RSS method with respect to the technique based on absolute RSS values plus calibration stage. Thus, the improvement is mainly related to the fact that the calibration stage is avoided, therefore allowing fast deployment of the ILS in the scenario.

Next, from the comparison of RSS-based ILS, inertial sensor positioning, and combination of RSS and inertial sensor, one may think that the inertial system is just slightly worse than the combined one, but the inertial system has a cumulative error that cannot be corrected unless combined with an absolute positioning system as the RSS-based technique.

The location method presented in this work has been compared in Table 1 with other RSS-based ILS and hybrid methods. If only RSS information is considered, the location error is in the same order as the cited RSS-based ILS's for a given scenario size and number of reference nodes. It is true that the proposed hybrid method is not as good as the proposed hybrid RFID-inertial system presented in Jiménez-Ruiz et al. (2012), but both are able to improve the results of RSS-based techniques, regardless the supporting technology (RFID, Huang et al., 2015; ZigBee, Gomes and Sarmento, 2009; Pivato et al., 2011; WiFi, Hossain et al., 2007; Ismail et al., 2008; Bluetooth, Bandara et al., 2004; Hossain et al., 2007). In addition, the interest on the proposed ILS lies on the ease of deployment and low cost, together with the capability of extending ZigBee coverage network beyond the range of a single static node thanks to the use of repeater

nodes, thus making it suitable for applications such as machinery, equipment or cargo tracking in industrial warehouses. A potential practical scenario could be cargo containers location and tracking in a sorting and storage facility in a seaport.

## Acknowledgements

This work has been supported by the ‘ministerio de Economía y Competitividad’ of Spain/European regional development fund (ERDF) under project TEC2014-54005-P (MIRIEM) and by the ‘Gobierno del principado de asturias’, asturias (Spain), under project GRUPIN14-114.

## References

- Accelerometer LIS331DLH (2015) *Manufacturer: ST*, [http://www.st.com/web/catalog/sense\\_power/FM89/SC444/PF218132](http://www.st.com/web/catalog/sense_power/FM89/SC444/PF218132) (Accessed 25 July, 2015).
- Álvarez, Y., de Cos, M.E., Lorenzo, J. and Las Heras, F. (2011) ‘Evaluation of an RSS-based indoor location system’, *Sensors and Actuators A: Physical*, Vol. 167, No. 1, pp.110–116.
- Bandara, U., Hasegawa, M., Inoue, M., Morikawa, H. and Aoyama, T. (2004) ‘Design and implementation of a Bluetooth signal strength based location sensing system’, *2004 IEEE Radio and Wireless Conference*, Atlanta, USA, pp.319–322.
- Chen, R.C., Huang, S.W., Lin, Y.C. and Zhao, Q.F. (2015) ‘An indoor location system based on neural networks and genetic algorithms’, *International Journal of Sensor Networks*, Vol. 19, Nos. 3–4, pp.204–216.
- Diebel, J. (2006) *Representing Attitude: Euler Angles, Unit Quaternions, and Rotation Vectors*, Stanford University, 94301-9010, 20 October, 2006, [https://www.astro.rug.nl/software/kapteyn/\\_downloads/attitude.pdf](https://www.astro.rug.nl/software/kapteyn/_downloads/attitude.pdf)
- Farid, Z., Nordin, R. and Ismail, M. (2013) ‘Recent advances in wireless indoor localization techniques and system’, *Journal of Computer Networks and Communications*, pp.1–12. AUTHOR PLEASE SUPPLY VOLUME NUMBER.
- Gallagher, T., Wise, E., Li, B., Dempster, A.G., Rizos, C. and Ramsey-Stewart, E. (2012) ‘Indoor positioning system based on sensor fusion for the Blind and Visually Impaired’, *3rd International Conference on Indoor Positioning and Indoor Navigation (IPIN’12)*, Sydney, Australia, Vol. 13, pp.1–9.
- Gomes, G. and Sarmiento, H. (2009) ‘Indoor location system using ZigBee technology’, *2009 Third International Conference on Sensor Technologies and Applications (SENSORCOMM’09)*, Athens/Glyfada, Greece, pp.152–157.
- Gyroscope L3GD20H (2015) *Manufacturer ST*, [http://www.st.com/web/en/catalog/sense\\_power/FM89/SC1288/PF254039](http://www.st.com/web/en/catalog/sense_power/FM89/SC1288/PF254039) (Accessed 25 July, 2015).
- Hossain, A.K., Nguyen Van, H., Jin, Y. and Soh, W.S. (2007) ‘Indoor localization using multiple wireless technologies’, *Fourth IEEE International Conference on Mobile Ad-hoc and Sensor Systems (MASS 2007)*, Pisa, Italy, pp.1–8.
- Huang, C.H., Lee, L.H., Ho, C.C., Wu, L.L. and Lai, Z.H. (2015) ‘Real-Time RFID indoor positioning system based on kalman-filter drift removal and heron-bilateration location estimation’, *IEEE Transactions on Instrumentation and Measurement*, Vol. 64, No. 3, pp.728–739.
- Ismail, M.B., Boud, A.F.A., and Ibrahim, W.N.W. (2008) ‘Implementation of location determination in a wireless local area network (WLAN) environment’, *Proceedings of the 10th International Conference on Advanced Communication Technology (ICACT’2008)*, Gangwon-Do, South Korea, Vol. 2, pp.894–899.
- Jiménez-Ruiz, A.R., Seco-Granja, F., Prieto-Honorato, J.C. and Guevara-Rosas, J.I. (2012) ‘Accurate pedestrian indoor navigation by tightly coupling foot-mounted IMU and RFID measurements’, *IEEE Transactions on Instrumentation and Measurement*, Vol. 61, No. 1, pp.178–189.
- Macii, D., Colombo, A., Pivato, P. and Fontanelli, D. (2013) ‘A data fusion technique for wireless ranging performance improvement’, *IEEE Transactions on Instrumentation and Measurement*, Vol. 62, No. 1, pp.27–37.
- Pivato, P., Palopoli, L. and Petri, D. (2011) ‘Accuracy of RSS-based centroid localization algorithms in an indoor environment’, *IEEE Transactions on Instrumentation and Measurement*, Vol. 60, No. 10, pp.3451–3460.
- Shirehjini, A.A.N., Yassine, A. and Shirmohammadi, S. (2012) ‘An RFID-based position and orientation measurement system for mobile objects in intelligent environments’, *IEEE Transactions on Instrumentation and Measurement*, Vol. 61, No. 6, pp.1664–1675.
- Sklar, B. (2001) *Digital Communications: Fundamentals & Applications*, 2nd ed., Prentice-Hall, USA, ISBN 0-13-084788-7.
- Tennina, S., Di Renzo, M., Graczioli, F. and Santucci, F. (2009) ‘ESD: a novel optimization algorithm for positioning estimation of WSNs in GPS-denied environments – from simulation to experimentation’, *International Journal of Sensor Networks*, Vol. 6, Nos. 3–4, pp.131–156.
- XBee® ZigBee RF Modules (2015) *Manufacturer: Digi*, <http://www.digi.com/products/xbec-rf-solutions/modules> (Accessed 25 July, 2015).

## Note

<sup>1</sup>Sklar (2001) and Huang et al. (2015) use power levels ( $P$ ) instead of field levels ( $E$ ):  $P_{Rx} = P_{ref} (\lambda/4\pi R)^2$ .